Separation and Purification Technology 156 (2015) 1064–1072

Contents lists available at ScienceDirect

Separation and Purification Technology

journal homepage: www.elsevier.com/locate/seppur

Efficient selenate removal by zero-valent iron in the presence of weak magnetic field

Liping Liang [b], Xiaohong Guan [a,*], Yuying Huang [c,*], Jingyuan Ma [c], Xueping Sun [c], Junlian Qiao [a], Gongming Zhou [a]

[a] State Key Laboratory of Pollution Control and Resources Reuse, College of Environmental Science and Engineering, Tongji University, Shanghai, PR China
[b] College of Life Science, Shaoxing University, Shaoxing, PR China
[c] Shanghai Synchrotron Radiation Facility, Shanghai Institute of Applied Physics, Chinese Academy of Sciences, Shanghai, PR China

ARTICLE INFO

Article history:
Received 4 February 2015
Received in revised form 16 July 2015
Accepted 24 September 2015
Available online 26 September 2015

Keywords:
Selenate
Reduction
Adsorption
Corrosion products
Lepidocrocite

ABSTRACT

Se(VI) was very refractory to be removed by zero-valent iron (ZVI), therefore weak magnetic field (WMF) was employed to achieve efficient Se(VI) removal by ZVI. Batch experiments showed that negligible Se (VI) (<4%) was removed by ZVI without the application of WMF within 72 h. The presence of WMF dramatically enhanced Se(VI) sequestration by ZVI and complete removal of 10.0 mg L^{-1} Se(VI) was achieved by ZVI in 90 min. The main portion of kinetics of Se(VI) removal by ZVI in the presence of WMF followed zero-order rate law and the rate constants of Se(VI) sequestration by ZVI increased progressively with increasing the ZVI dosage. Fe *K*-edge XAFS spectra and synchrotron radiation-XRD analysis revealed that ZVI was transformed to X-ray amorphous Fe_3O_4 before finally transformed to lepidocrocite (γ-FeOOH). The LCF analysis of Se *K*-edge XANES spectra indicated that adsorptive removal of Se(VI) was minor but adsorption of Se(VI) to the corroded ZVI surface was the first step of Se(VI) removal. Se(VI) was rapidly reduced to Se(IV), which could be further transformed to Se(0). Comparison of the performance of Se(VI) removal in the literature suggested that employing WMF to enhance Se(VI) removal by ZVI under oxic conditions be a promising method.

1. Introduction

Selenium is an environmental pollutant and ranks 147th on the Superfund Priority List of Hazardous Substances of the U.S. Comprehensive Environmental Response, Compensation, and Liability Act (CERCLA) [1]. Depending on its concentration, selenium can act as an essential micro-nutrient protecting against reactive oxygen species damages, or as a toxic compound [2]. Se pollution is a worldwide problem and mainly originates from agricultural practices, manufacture processes, coal combustion and mining processes [3]. Se was found to be present in elevated concentrations in acid mine drainage which varied from 1 to 7000 μg L^{-1} [4].

Selenium (Se) is a metalloid that exists in a variety of oxidation states including selenide (Se(-II)), elemental Se (Se(0)), selenite (Se (IV)), and selenate (Se(VI)) [5]. The oxidized forms of Se, Se(VI) and Se(IV), are soluble and mobile and thus are potentially toxic [6]. Selenite is similar to phosphate in terms of mobility in the environment and tends to be adsorbed more strongly than selenate onto adsorbents such as goethite and hematite [7,8]. However, selenate, similar to sulfate, is very difficult to be adsorbed on various minerals. Thus, it is the most mobile selenium species and very difficult to be removed by the conventional methods including coagulation, lime softening and adsorption [9]. Compared to the above Se(VI) removal methods, reductive removal by zero-valent iron (ZVI) should be more favored since ZVI is a readily available, inexpensive, and moderately strong reducing agent and can transform Se (VI) to the more immobile species, Se(IV), Se(0) or Se(-II) [3].

Several studies had been carried out to examine the performance of ZVI toward Se(VI) removal. However, the iron filings or microscale iron powder had low reactivity toward Se(VI) removal. A huge dosage of micron-sized ZVI (50–100 g L^{-1}) was necessary to sequester Se(VI) and the removal capacity of ZVI for Se(VI) was very low [2,10]. To improve the removal rate of Se(VI) by ZVI, nano-sized ZVI (nZVI) and NiFe bimetal were used [11]. Moreover, Tang et al. [12,13] proposed to apply Co^{2+}, Mn^{2+} or Fe^{2+} to improve Se(VI) removal by ZVI. However, both methods bear some demerits. Although iron is inexpensive in bulk form, nZVI and nano-sized NiFe bimetal were much more expensive because the costly precursor reagents and complicated processes are needed to synthesize them [14]. Furthermore, the toxicity of nanomaterial

* Corresponding authors.
E-mail addresses: guanxh@tongji.edu.cn (X. Guan), huangyuying@sinap.ac.cn (Y. Huang).

http://dx.doi.org/10.1016/j.seppur.2015.09.062
1383-5866/

has arisen much concern [15] and Lee et al. [16] reported that nZVI showed a strong bactericidal activity comparable to that of silver nanoparticles. Although Tang et al. [12,13] did show that the application of Co^{2+}, Mn^{2+} or Fe^{2+} could greatly enhance Se(VI) by ZVI, a ZVI dosage as high as 50.0 g L^{-1} was employed in their study to removal 20.0 mg L^{-1} Se(VI) and the dosing of Co^{2+} or Mn^{2+} may induce secondary pollution. Therefore, it is critical to explore an environmentally friendly method that can significantly improve the reactivity of ZVI to remove Se(VI).

Our recent studies reported that the application of a weak magnetic field (WMF) could greatly accelerate ZVI corrosion and sequestration of Se(IV), As(III), and As(V) [17–19]. The primary role of WMF in the process of contaminants removal by ZVI was to enhance mass transfer [19]. Up to now, no study had been performed on the influence of WMF on Se(VI), which was much more refractory than Se(IV), removal by ZVI. However, two studies [11,20] on Se(VI) removal by ZVI, which employed magnetic stirrer to offer mixing, showed much more efficient Se(VI) removal by ZVI than other studies. The magnetic field generated by the magnetic stirrer was stronger than the WMF applied in our previous studies [18], thus it was expected that WMF had promoting effect on Se (VI) removal by ZVI. Therefore, the current work was aimed at investigating the kinetics and mechanisms of Se(VI) removal from water by ZVI in the presence of WMF.

2. Materials and methods

2.1. Materials

All chemicals were analytical grade and used as received. The high purity ZVI powders (99.8–99.9% Fe^0), with d_{50} of 7.4 μm and BET specific surface area (a_s) of 0.3015 m^2 g^{-1}, were purchased from Beijing Dk Nano technology Co., LTD, and used in this study without further treatment. Chemicals including $Na_2SeO_4{\cdot}10H_2O$, HCl, NaOH and 2-(N-morpholino)ethanesulfonic acid (MES) were purchased from Shanghai Qiangshun Chemical Reagent Company and were used as received in this study. The stock solutions were prepared by dissolving the corresponding salts in ultrapure water generated from a Milli-Q Reference water purification system.

2.2. Batch experiments and chemical analysis

To investigate the feasibility of Se(VI) removal by ZVI in the presence of WMF, the experimental setup employed in our previous study was also used here [18]. In brief, two cylindrical neo dymium–iron–boron permanent magnets with diameter of 30 mm and height of 5 mm on an iron sheet were placed under the reactor, which provided a maximum magnetic field intensity of 20 mT at the bottom of the reactor throughout the course of the experiment [18]. Batch tests were carried out in 500 mL glass bottles and the solutions were open to the air or purged with nitrogen gas during continuous mixing with mechanical stirring (310 rpm). The aqueous medium consisted of Se(VI), 0.01 M NaCl and 0.1 M MES as buffer to keep pH constant (6.0 ± 0.1). MES was employed as buffer because it did not form complexes with Fe^{2+} or Fe^{3+} [21]. The tests were initiated by adding 1.0 g L^{-1} of ZVI. All experiments were performed at 25 °C, which was controlled with a water bath. At fixed time intervals, aliquots of 5 mL sample were periodically withdrawn from the center of the reactor by a Teflon tube connected to a plastic syringe and immediately filtered with a 0.22 μm pore diameter membrane. Hereafter the extracted samples were acidified and analyzed for residual Se(VI) concentration with Perkin Elmer Optima 5300 DV ICP–OES. Fe^{2+} concentration in the filtrate was determined by the modified ferrozine method using a TU-1901 UV/visible spectrophotometer at a wavelength of 562 nm following the procedure of Stookey [22]. The Oxidation Reduction Potential (ORP) of each sample was monitored with an ORP sensor connected to a pHS-3C pH meter. All experiments were carried out in triplicates for a given condition, and all points in the figures are averaged and error bars represent the standard deviation.

2.3. Solid phase characterization

The reacted ZVI samples were collected at different intervals, washed with distilled water, freeze-dried and put into zippered bags before subjecting to Se *K*-edge and Fe *K*-edge X-ray Absorption Fine Structure (XAFS) analysis. XAFS analysis was performed at BL14 W Beam line at Shanghai Synchrotron Radiation Facility (SSRF) (Shanghai, China). The details of XAFS analysis are present in Text S1 of Supporting Information [23].

The X-ray diffraction data of the ZVI samples reacted with Se (VI) were obtained at beamline BL14B1 of the Shanghai Synchrotron Radiation Facility (SSRF) at a wavelength of 1.2398 Å. BL14B1 is a beamline based on bending magnet and a Si(111) double crystal monochromator was employed to monochromatize the beam. The size of the focus spot is about 0.5 mm and the end station is equipped with a Huber 5021 diffractometer. NaI scintillation detector was used for data collection.

3. Results and discussion

3.1. Effect of initial Se(VI) concentrations

As illustrated in Fig. 1(a), negligible Se(VI) (<4%) was removed by ZVI without the application of WMF within 72 h, regardless of the initial Se(VI) concentration varying from 10.0 to 100.0 mg L^{-1}. Similar phenomenon had been reported by Tang et al. [13] although ZVI dosage as high as 50 g L^{-1} was employed in their study. In our previous study [18], it took only 60 min to achieve almost complete removal of Se(IV) of 40.0 mg L^{-1} by the same ZVI sample under similar conditions. Obviously, the reductive removal of Se(IV) was much more facile than that of Se(VI) although the redox potential of the $SeO_4^{2-}/HSeO_3^-$ couple was larger than that of the $HSeO_3^-/Se^0$ couple, as shown in Eqs. (1) and (2) [24]. Selenite is a softer base than selenate [25] and thus has smaller resistance to electron transfer and is more reactive with Fe^0 [26].

$$SeO_4^{2-} + 2e^- + 3H^+ \rightarrow HSeO_3^- + H_2O \quad E^0 = 1.15\ V \tag{1}$$

$$HSeO_3^- + 4e^- + 5H^+ \rightarrow Se^0 + 3H_2O \quad E^0 = 0.74\ V \tag{2}$$

The superimposed WMF remarkably improved Se(VI) sequestration by ZVI, as illustrated in Fig. 1(b). It was surprising to find that 10.0 mg L^{-1} Se(VI) could be completely sequestered by 1.0 g L^{-1} ZVI in 90 min in the presence of WMF. The removal efficiencies were 96.3%, 67.6% and 36.9% after 12 h of reaction, respectively, when the initial Se(VI) concentrations were 20.0, 40.0, and 100.0 mg L^{-1}. Moreover, Se(VI) removal by ZVI with WMF was almost completed within 5 h when the initial Se(VI) concentration was in the range of 20.0–100.0 mg L^{-1} and negligible removal of Se (VI) was observed with prolonged reaction time. The main portion of each data set in Fig. 1(b) could be well described by the zero-order kinetics. The fitting results are presented with dotted lines in Fig. 1(b). It was found that the zero-order rate constants (k_{obs}) were in the range of 0.094–0.141 mg L^{-1} min^{-1}, no obvious dependence on the initial concentration of Se(VI).

The variations of Fe^{2+} concentration and ORP with time in the process of Se(VI) removal by Fe^0 were also examined and present in Fig. 1(c) and (d), respectively. ZVI reacted with Se(VI) solution

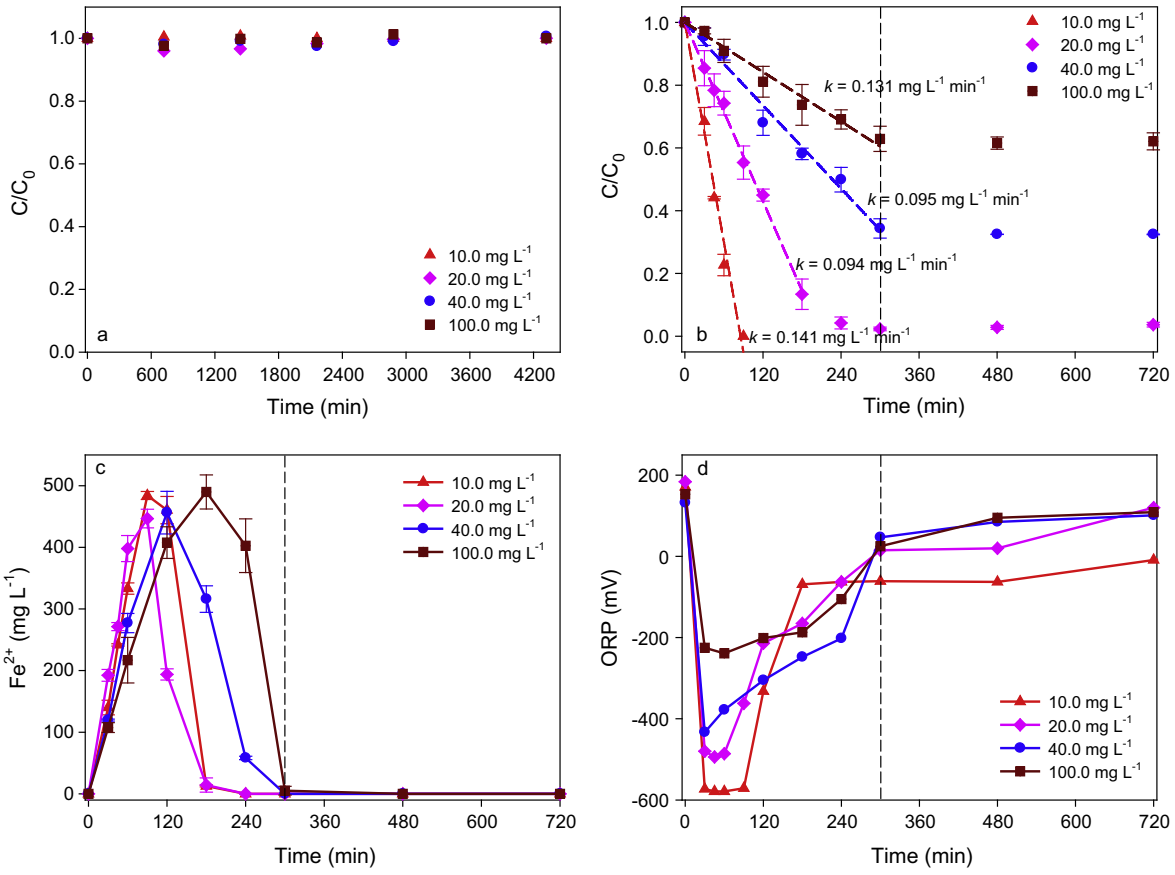

Fig. 1. Concentration profiles of dissolved Se(VI) in the absence of WMF (a) and those in the presence of WMF (b); Concentration profiles of dissolved Fe^{2+} (c) and variation of ORP in the process of Se(VI) removal by ZVI in the presence of WMF. The dotted lines in (b) are the results of simulating the kinetics Se(VI) removal by ZVI in the presence of WMF with zero-order rate law. ($[Se(VI)]_0$ = 10.0–100.0 mg L^{-1}, ZVI = 1.0 g L^{-1}, NaCl = 0.01 M, pH = 6.0).

underwent dissolution and the Fe^{2+} concentration increased almost linearly with time to 446–489 mg L^{-1}, which corresponded well with the observed zero-order kinetics of Se(VI) removal by ZVI with WMF. Hereafter, the concentration of Fe^{2+} dropped sharply to near zero, which should be ascribed to the oxidation of aqueous Fe^{2+} by dissolved oxygen, similar to the phenomena reported in our previous studies [5,18,19]. As shown in Fig. 1(d), the initial ORP values were in the range of 150–200 mV and they dropped abruptly to −579 ∼ −240 mV in the first 30 min and then gradually increased to −61 ∼ 40 mV at 5 h. Comparing the trend of ORP variation and that of Fe^{2+} concentration, the gradual increase in ORP after 5 h should be mainly associated with the increase of dissolved oxygen. ORP is a mixed potential (E_{mix}) composed of the weighted sum of Nernstian terms for each of the redox couples that are present at the electrode surface [27]. In the process of Se(VI) removal by ZVI open to the air, redox couples (Red_i and Ox_i) that contribute to ORP values mainly include H_2/H^+, OH^-/O_2, Fe^0/Fe^{2+} as well as $HSeO_3^-/SeO_4^{2-}$ [27]. The lowest ORP values observed in the process of Se(VI) removal by ZVI with WMF increased with increasing initial Se(VI) concentration, which could be ascribed to the higher residual Se(VI) concentration at higher initial Se(VI) concentration.

3.2. Effect of ZVI dosage

The influence of ZVI dosages on Se(VI) removal rate was investigated with initial Se(VI) concentration of 40.0 mg L^{-1} at pH 6.0 in the presence of WMF, as shown in Fig. 2. Obviously, the removal rate of Se(VI) was increased with increasing ZVI dosage, as demonstrated in Fig. 2(a). Only 65.6% of Se(VI) was removed by 1.0 g L^{-1} ZVI in 3 h. With increasing the ZVI dosage to 1.5 and 2.0 g L^{-1}, 90.7% and 99.4% of Se(VI) were removed from the solution during 5 h of mixing, respectively. Complete removal of Se(VI) by 2.5 g L^{-1} ZVI could be achieved in 4 h. Similar to the phenomenon present in Fig. 1(b), Se(VI) removal experienced two stages at ZVI dosage of 1.0–2.0 g L^{-1}, a rapid stage and a slow stage hereafter. Se(VI) removal at various ZVI dosages followed zero-order rate law during the rapid removal stage. The zero-order rate constants of Se(VI) removal increased linearly from 0.088 to 0.236 mg L^{-1} min^{-1} as the ZVI dosage was increased from 1.0 to 2.5 g L^{-1}, as illustrated in Fig. 2(b). Increasing the applied ZVI dosage, more available active sites were available for Se(VI) rapid adsorption and reduction, resulting in higher removal rate [28]. Furthermore, the maximum concentration of soluble Fe^{2+} increased and the lowest ORP dropped with increasing ZVI dosage, as shown in Fig. 2(c) and (d), respectively. The Fe^{2+} concentrations increased almost linearly with time reaching values of 456.2, 645.6, 792.4, 858.9 mg L^{-1}, respectively, when ZVI were dosed at 1.0, 1.5, 2.0, and 2.5 g L^{-1}. Although there was still 157 mg L^{-1} Fe^{2+} after 5 h of reaction when ZVI was applied at 1.5 g L^{-1}, negligible Se(VI) was removed after 5 h even there was still 9.3% Se(VI) residual in the solution, indicating that Fe^{2+} was not an effective electron donor for reductive removal of Se(VI) [29]. Klas and Kird [30] reported that the electron donor for Se(VI) reduction was not Fe^0 but a reactive Fe^{2+}-bearing solid formed during oxidation of Fe^0 by O_2, thus more rapid Se(VI) removal by ZVI was observed under oxic conditions, which did not agree with our observations. Because more Fe^{2+} was generated, more oxygen was consumed and less Se(VI) was residual at higher ZVI dosage, ORP dropped to a greater extent and rebound more slowly at higher ZVI dosage, as shown in Fig. 2(d). The results present in Figs. 1 and 2 suggested

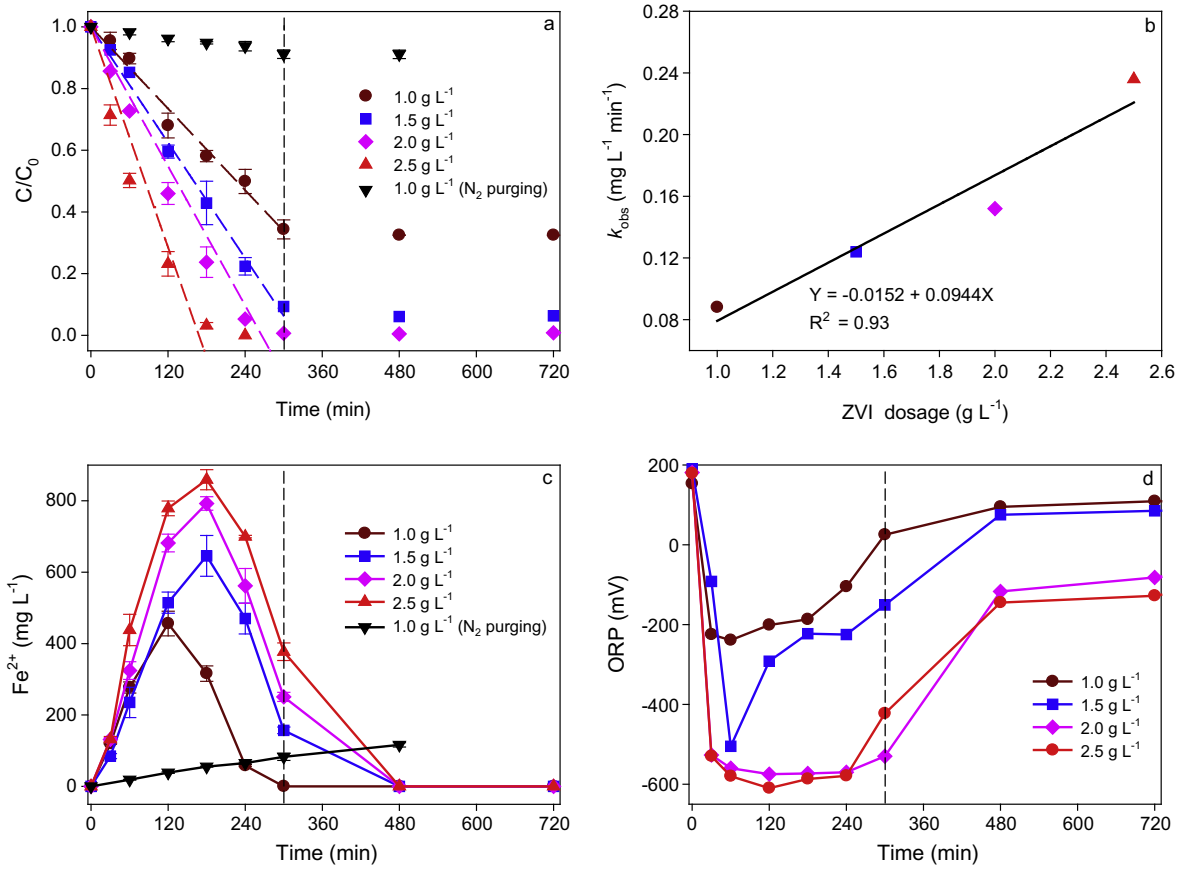

Fig. 2. Influence of ZVI dosage on (a) the concentration profiles of dissolved Se(VI), (c) the concentration profiles of dissolved Fe^{2+}, and (d) variation of ORP in the process of Se (VI) removal by ZVI in the presence of WMF. The dotted lines in (a) are the results of simulating the kinetics Se(VI) removal by ZVI in the presence of WMF with zero-order rate law and (b) shows the correlation between the zero-order rate constants of Se(VI) removal by ZVI ($[Se(VI)]_0$ = 40.0 mg L^{-1}; ZVI = 1.0–2.5 g L^{-1}; NaCl = 0.01 M, pH = 6.0). The dots (▼) in (a) and (b) stand for kinetics of Se(VI) removal and the generation of Fe^{2+} in the process of Se(VI) removal by ZVI, respectively, under N_2 purging condition.

that the negligible removal of Se(VI) after 5 h should be associated with the almost exhaustion of Fe^0, which will be verified by the XAFS analysis in Section 3.4.

3.3. Comparison of the treatment technologies for Se(VI) removal

Selenate is a weakly basic group VI oxyanion and typically exists in natural aqueous systems as the fully deprotonated form (SeO_4^{2-}). Since SeO_4^{2-} is a hard base, it has low affinity for various metal (hydr)oxides and generally adsorbed by forming outer-sphere complexes [31]. A variety of treatment technologies had been investigated for Se(VI) removal and the most two common methods are adsorption and abiotic reduction. Table 1 summarizes the removal capacities of SeO_4^{2-} in adsorption and abiotic reduction processes as well as the reaction conditions under which the experiments were performed. It was found that the adsorption capacity of SeO_4^{2-} on various adsorbents was always very low and varied from 0.24 to 15.12 mg g^{-1}. In addition, the adsorption of SeO_4^{2-} dropped progressively with increasing pH and strongly influenced by the co-existing solutes including sulfate [32]. Therefore, removal of Se(VI) from water by adsorption is not a wise option.

Taking advantage of the reducible property of Se(VI), removal of Se(VI) by photocatalytic reduction, electrochemical reduction, and reduction with Fe^{2+}-containing materials, ZVI or nZVI had been investigated in the literature, as summarized in Table 1. To achieve Se(VI) reduction in photocatalytic process, excessive organic reductant, e.g., formic acid, had to be employed [33], but the organic reductant could not be completely mineralized in this process thus leading to secondary pollution. The reduction rate of selenate increases with increasing the applied current and with decreasing the initial concentration of selenate in the electrochemical system [24]. However, the scale-up of electrochemical method is very difficult. Compared to photocatalytic and electrochemical reduction, reductive removal of Se(VI) by ZVI or nZVI is more flexible and easily applicable. Although nZVI had good performance toward Se(VI) sequestration, it was much more expensive than the micron-sized ZVI [34] and its toxicity on to humans and biota had arisen much concern [35]. Compared to the capacities of Se(VI) removal (0.02–2.76 mg g^{-1}) by micron-sized ZVI listed in Table 1, much more efficient Se(VI) removal (36.9 mg g^{-1}) was observed in our study, which should be because the experiments were carried out open to the air and in the presence of WMF. Under N_2 purging conditions, less than 10% of Se(VI) was removed by ZVI in 8 h even in the presence of WMF, as demonstrated in Fig. 2(a), consistent with the results reported by Klas and Kird [30] and Yoon et al. [20]. In their studies, magnetic stirrer was employed to offer mixing and thus WMF was introduced by the magnetic stirrer in their studies although the authors did not notice the WMF effect on Se(VI) removal by ZVI. Moreover, these two studies reported an enhancing effective of dissolved oxygen on the removal rate of Se(VI) by ZVI. Therefore, the above discussion revealed that Se (VI) removal by ZVI coupling with WMF open to the air was a promising method compared with those reported in the literature.

3.4. Fe K-edge XAFS spectra

The Fe *K*-edge XANES spectra and k^3-weighted EXAFS spectra of ZVI particles reacted with 40.0 mg L^{-1} Se(VI) open to air at pH 6.0

Table 1
Summary of selenate removal capacity by adsorption or abiotic reduction.

Technology	Materials	Initial Se(VI) concentration (mg L^{-1})	Dosage of adsorbent or reductant (g L^{-1})	pH	Reaction time (h)	Removal capacity[d] (mg g^{-1})	Reference
Adsorption	Iron-coated granular activated carbons	1.0	3.5	5.0[a]	48.0	0.39	[9]
	Nano-Jacobsite	0.1	2.5	4.0[a]	0.25	0.77	[36]
	Goethite	0–94.8	10.0	6.0[b]	24.0	2.50	[37]
	Hematite	0.24–39.48	10.0	4.0[c]	50.0	0.24	[38]
	γ-Al_2O_3	394.8	30.0	2.0[c]	24.0	10.42	[32]
	Hydrous aluminum oxide	7.90	0.5	6.0[a]	48.0	14.76	[39]
	Corundum	0.40	1.25	6.0[a]	48.0	0.59	[39]
	Magnetite	0.24–39.48	5.0	4.0[a]	30.0	0.25	[40]
	Magnetic nano-particle–graphene oxide (MGO) composites	0–100	1.0	6.0[b]	24.0	15.12	[41]
	Ferrihydrite	8.0	4.0	7.0[b]	24.0	2.00	[42]
	Aluminum-oxide-coated sand	0–157.9	100.0	4.9[a]	3.0	0.92	[43]
	Microwave-assisted Fe_3O_4	0.1	2.5	4.0[b]	1.0	2.37	[44]
Abiotic reduction	Green rust	536.9	[T-Fe]=79.8 mM	7.5[a]	11.0	42.10	[6]
	Photocatalytic reduction	106.7	[HCOOH]=10 mM, [TiO_2]=1.1 g L^{-1}	7.6[a]	5.0	45.30	[33]
	Photocatalytic reduction	20.0	[HCOOH]=25 mM, [Ag-TiO_2]=0.5 g L^{-1}	3.5	4.5	~100%*	[33]
	Electrochemical	31.6	[bicarbonate]=10 mM, 90 mA	7.0[b]	6.0	45.1%*	[24]
	ZVI	1.0	50.0	5.9[b]	1.0	0.02	[10]
	ZVI	300.0	100.0	6.0[b]	120	2.76	[2]
	ZVI + Co^{2+}	20.0	Fe^0: 50 g L^{-1}, Co^{2+}: 59 mg L^{-1}	6.2[b]	3	0.40	[12]
	ZVI + Fe^{2+}	20.0	Fe^0: 50 g L^{-1}, Fe^{2+}: 28 mg L^{-1}	–	11	0.40	[13]
	Nano-ZVI	237.0	1.5	8.0–8.2[c]	48	138.25	[3]
	Nano-NiFe	103.0	1.0	7.7[b]	5.0	83.4†	[11]
	Nano-ZVI	100.0	1.0	7.7[b]	5.0	65.88†	[11]
	ZVI with WMF	100.0	1.0	6.0[a]	5.0	36.9	This study

* The removal efficiency.
[a] Keep pH constant.
[b] Initial pH.
[c] pH at equilibrium.
[d] Adsorption capacity or removal capacity (the maximum amount of Se(VI) removed by each gram ZVI under the investigated experimental conditions).
† Mixed with magnetic stirrer.

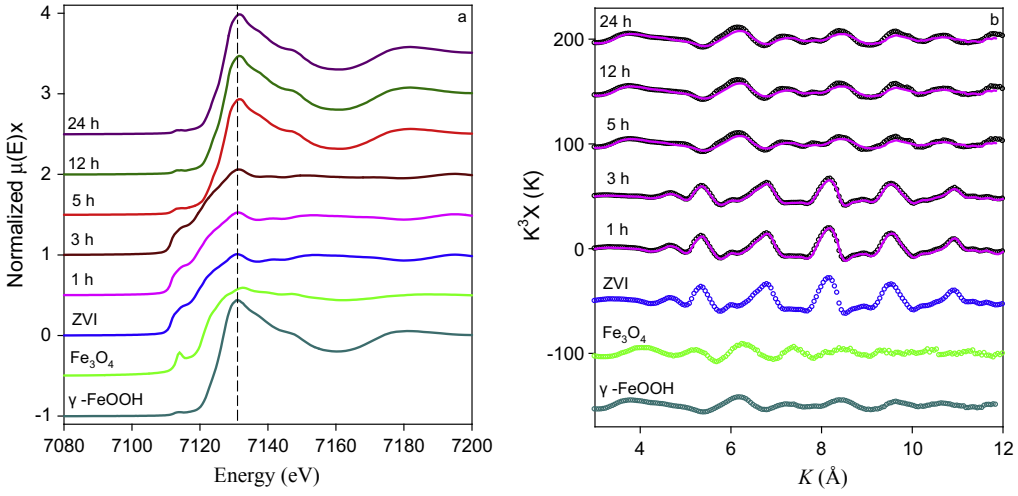

Fig. 3. Fe *K*-edge XANES spectra (a) and k^3-weighted EXAFS spectra (b) of Se(VI)-treated ZVI corrosion products and reference materials (ZVI = 1.0 g L^{-1}, $[Se(VI)]_0$ = 40.0 mg L^{-1}, NaCl = 0.01 M, pH = 6.0). Experimental data in (b) are shown as empty circles and the solid lines in (b) stand for the linear combination fitting results.

in the presence of WMF and the reference materials are shown in Fig. 3. To identify the Fe species in the collected samples, the linear component fitting (LCF) analysis was carried out based on the Fe k^3-weighted EXAFS spectra. The best LCF fits of the solid samples were shown with solid lines in Fig. 3(b) and the corresponding fitting results are shown in Fig. 4(a). The fraction of Fe^0 decreased rapidly from 100% to 6.8% within 5 h. The magnetite (Fe_3O_4) content gradually increased to 27.5% within 3 h and then dropped to 0% after 5 h. LCF analysis revealed that all Fe in the solid phase was present as lepidocrocite (γ-FeOOH) in the presence of WMF after 5 h.

Synchrotron radiation-XRD patterns of ZVI particles reacted with 40.0 mg L^{-1} Se(VI) open to air at pH 6.0 in the presence of WMF at different time were also collected, shown in Fig. 4(b). Only Fe^0 was identified in the samples collected at 1 h and 3 h but no XRD patterns corresponding to Fe_3O_4 were observed these samples, indicating that Fe_3O_4 detected by XAFS in these samples was disordered and X-ray amorphous. The XRD analysis confirmed that the ZVI particles were completely transformed to lepidocrocite (JCPDS 74-1877) in the time scale of our study as shown in Fig. 4(b). Combining the results of the XRD and XAFS analysis, it was concluded that Fe^0 was sequentially transformed to Fe_3O_4 and

then to γ-FeOOH in the process of Se(VI) removal by ZVI with WMF, which was similar to what reported in the previous studies [19,45] and could be described by Eqs. 3–5.

$$2Fe^0 + O_2 + 2H_2O \rightarrow 2Fe^{2+} + 4OH^- \quad (3)$$

$$6Fe^{2+} + O_2 + 6H_2O \rightarrow 2Fe_3O_4 + 12H^+ \quad (4)$$

$$4Fe^{2+} + O_2 + 6H_2O \rightarrow 4\gamma\text{-FeOOH} + 8H^+ \quad (5)$$

3.5. Se K-edge XANES spectra

To obtain direct evidence for the mechanisms of selenate removal by ZVI in the presence of WMF, the Se *K*-edge XANES spectra of 1.0 g L^{-1} ZVI particles reacted with 40.0 mg L^{-1} Se(VI) for different time in the presence of WMF were collected and shown in Fig. 5(a). LCF analysis of these Se *K*-edge XANES spectra was carried out to semi-quantitatively identify the Se species in the collected samples and the results are summarized in Table S1. A variety of standards (selenium powder for Se(0); iron selenite ($FeSeO_3$) for Se(IV); sodium selenate (Na_2SeO_4)) were tested as possible components of the unknown, and the fitting results using iron selenite were superior to those using sodium selenite. The major Se phases in Se(VI)-treated ZVI samples within 3 h were Se(0) and Se(IV). Moreover, the fraction of Se(IV) gradually decreased from 28.0 ± 0.013% to 12.9 ± 0.013% as time elapsed from 15 min to 180 min, and concomitantly the fraction of Se(0) gradually elevated from 74.3 ± 0.013% to 89.0 ± 0.012%. However, no evidence suggesting the formation of a crystalline Se-containing phase was observed in our XRD data, as shown in Fig. S1(b). Therefore, it is likely that a poorly crystalline Se-containing phase was present in a mixture with iron (hydr)oxides [5]. No Se(VI) was detected in the precipitates in the first 3 h of the reaction while it appeared in the precipitates collected after reacted with Se(VI) for 5 h, which was accompanied with a slight decrease in the Se(0) fraction to 82.9 ± 0.016% in the precipitates. Se(VI) consisted of less than 10% of the total removed Se in the precipitates at the end of 24 h although the concentration of Se(VI) residual in aqueous phase was high. Moreover, the speciation of dissolved Se(VI)/Se(IV) determined by LC–ICP–MS (data not shown) indicated that only Se(VI) was present in the aqueous phase, consistent with the report by Olegario et al. [3].

Figs. 3 and 4 reveal that Fe_3O_4 and γ-FeOOH are the major corrosion products of ZVI in the process of Se(VI) removal by ZVI in the presence of WMF. It was well known that the adsorption of Se(VI) on iron (hydr)oxides including Fe_3O_4 and γ-FeOOH was weak and the adsorption capacity of iron (hydr)oxides for Se(VI) was small. However, the adsorption on and incorporation of Se(IV) into the corrosion products of ZVI was much more stronger than Se(VI) [46]. Considering the evidences provided by XAFS analysis and the adsorption properties of Se(VI) and Se(IV), the possible mechanisms of Se(VI) removal by ZVI in the presence of WMF are proposed to be as follows:

$$Fe^0 + SeO_4^- + 3H^+ \rightarrow Fe^{2+} + HSeO_3^- + H_2O \quad (6)$$

$$2Fe^0 + HSeO_3^- + 5H^+ \rightarrow 2Fe^{2+} + Se^0 + 3H_2O \quad (7)$$

Se(VI) was sequentially reduced by ZVI to Se(IV) and Se(0), following Eqs. (6) and (7). However, for these reductive reactions to occur, Se(VI) must be adsorbed onto the surface and then be reduced by electrons that are donated by ZVI. Therefore, it can be inferred that the reductive transformation of Se(VI) to Se(IV) and Se(0) was the driving force for the subsequent adsorption of Se(VI) onto the corroded ZVI surface. When Fe^0 was almost completely exhausted after 5 h, little Se(VI) was adsorbed on the corrosion products of ZVI and could not be further reduced.

The XANES spectra of 1.0 g L^{-1} ZVI particles reacted with 10.0, 20.0 and 100.0 mg L^{-1} Se(VI) for 24.0 h and those of 1.5, 2.0 and 2.5 g L^{-1} ZVI particles reacted with 40.0 mg L^{-1} Se(VI) at pH = 6.0 for 24.0 h in the presence of WMF were shown in Fig. 5(b). The corresponding LCF analysis results in Table S1 unraveled that all the removed Se(VI) were present as Se(0) and Se(IV), with the fraction of Se(0) being 78.4 ± 2.2% and that of Se(IV) being 21.6 ± 3.9%, at the end of 24.0 h reaction in the presence of WMF when the initial mass ratio of Se(VI) to Fe^0 was smaller than 40 mg/g. As the initial Se(VI) concentration was elevated to 100.0 mg L^{-1} (the initial mass ratio of Se(VI) to Fe^0 was 100 mg/g), Se(0), Se(IV) and Se(VI) coexisted in the precipitates collected at 24 h with their fractions being 55.8 ± 0.017%, 42.3 ± 0.016% and 11.5 ± 0.014%, respectively. The results of Se *K*-edge XANES spectra showed that the reductive transformation of Se(VI) to Se(IV) and Se(0) primarily contributed to Se(VI) sequestration by ZVI in the presence of WMF. The fractions of Se(IV) and Se(0) in the final products were determined by the initial mass ratio of Se(VI) to Fe^0. The coprecipitation and adsorption of Se(VI) by ZVI corrosion products only contributed

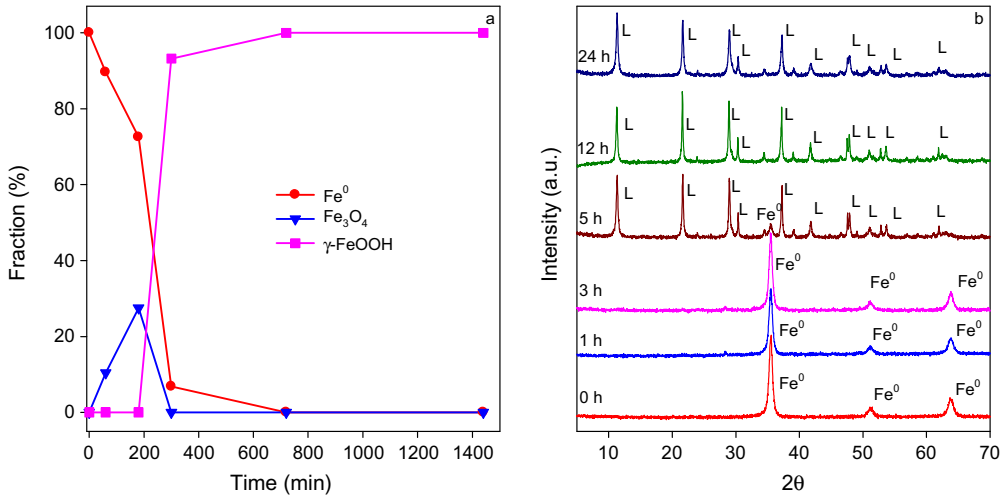

Fig. 4. (a) Fraction of Fe species in ZVI particles reacted with 40.0 mg L^{-1} Se(VI) open to air at pH 6.0 based on LCF of Fe k^3-weighted EXAFS spectra; (b) Synchrotron radiation-XRD patterns of ZVI particles reacted with 40.0 mg L^{-1} Se(VI) open to air at pH 6.0 in the presence of WMF (Fe^0 = 1.0 g L^{-1}).

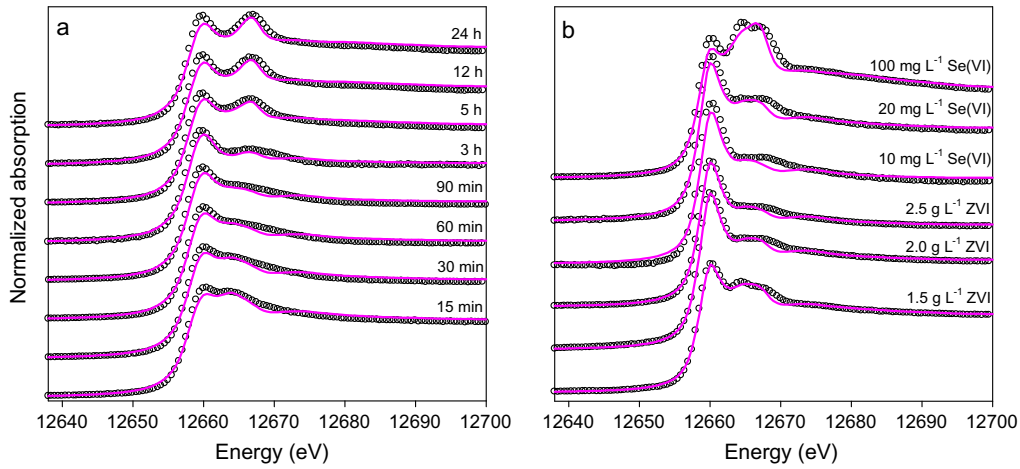

Fig. 5. (a) Se *K*-edge XANES spectra of 1.0 g L^{-1} ZVI particles reacted with 40.0 mg L^{-1} Se(VI) for different time in the presence of WMF; (b) XANES spectra of 1.0 g L^{-1} ZVI particles reacted with 10, 20 and 100.0 mg L^{-1} Se(VI), respectively, for 24 h in the presence of WMF, and of 1.5, 2.0 and 2.5 g L^{-1} ZVI particles reacted with 40.0 mg L^{-1} Se(VI) for 24 h (b). Experimental data are shown as empty circles. The solid lines represent the linear combination fits using the Se standard materials.

slightly to Se(VI) removal by ZVI in the presence of WMF. The proposed mechanisms of Se(VI) sequestration by ZVI in the presence of WMF are schematically illustrated in Fig. 6. Based on the results derived from the Fe and Se *K*-edge XAFS spectra, less than 5% of the electrons donated by Fe^0 were transferred to Se(VI) for its reductive removal in the presence of WMF, indicating that most of the Fe^0 was consumed by oxygen rather than Se(VI). The removal rate of Se(VI) was improved under oxic conditions compared to the case under anoxic conditions but the selectivity of Fe^0 toward the reductive removal of Se(VI) was deteriorated arising from the competition of oxygen.

In our study, formation of $FeSe_2$ and FeSe was not observed although several studies on Se(VI) removal by ZVI had reported the formation of $FeSe_2$ and FeSe. Olegario et al. [3] reported that Se(VI) was transformed to short-range ordered FeSe by nZVI. Yoon et al. [20] showed that Se(VI) was reduced by ZVI to Se(0) and Se(-II) at pH ranging from 4.0 to 10.0 when the initial Se(VI) concentration was 10.0 mg L^{-1}. At pH 6.0, Se(VI) could be completely reduced by ZVI to Se(0)/Se(-II) when the initial Se(VI) concentration was $\leqslant$25.0 mg L^{-1}. As the initial Se(VI) concentration was $\geqslant$50.0 mg L^{-1}, Se(VI) was only partially reduced to Se(0)/Se(-II) thus Se(VI) and Se(IV) were also present in the Se(VI)-treated ZVI samples. Their results were contradictory with those reported by Kang et al. [47], who demonstrated that Se(0) was the final reductive product Se(VI), especially when Se(IV) was also present because oxidation of FeSe by selenite is thermodynamically favorable and with relatively fast kinetics. Tang et al. [13] employed sequential extraction to identify the transformation of selenium species in the Se(VI)–ZVI–Fe^{2+} system after 24 h reaction and unraveled that Se(VI) disappeared from aqueous phase was transformed to adsorbed Se(VI) and Se(IV) and then to Se(0), consistent with our observations.

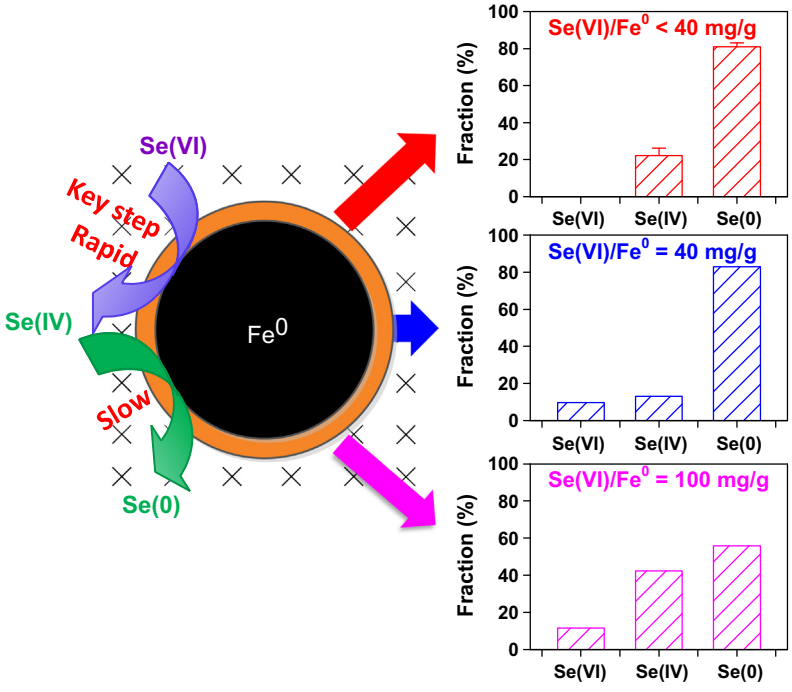

Fig. 6. Proposed mechanisms of Se(VI) sequestration by ZVI in the presence of WMF.

4. Conclusions

This study showed that Se(VI) could be effectively removed by ZVI in the presence of WMF at pH 6.0. With the application of WMF, 10.0 mg L^{-1} Se(VI) could be completely removed by 1.0 g L^{-1} ZVI in 90 min and 40.0 mg L^{-1} Se(VI) could be completely removed by 2.5 g L^{-1} ZVI in 4 h under oxic conditions. Se(VI) removal by ZVI in the presence of WMF was much more favored under oxic conditions than that under anoxic conditions. Fe *K*-edge and Se *K*-edge XAFS spectra indicated that Se(VI) was sequestered by adsorption to the corroded ZVI surface followed by fast reduction to Se(IV) and then to Se(0), with lepidocrocite as the final corrosion product of ZVI. The distribution of Se species in the ZVI samples reacted with Se(VI) was highly dependent on the initial mass ratio of Se(VI)/Fe^0. As the initial mass ratio of Se(VI)/Fe^0 was <40 mg g^{-1}, the removed Se(VI) was completely transformed to Se(IV) and Se(0). However, about 10% of the removed Se(VI) was not reduced when the initial Se(VI)/Fe^0 mass ratio was >40 mg g^{-1} and the fraction of Se(0) dropped with increasing the initial Se(VI)/Fe^0 initial mass ratio. This study verified that employing WMF to enhance Se(VI) removal by ZVI under oxic conditions was a promising and environmental-friendly method. The coupling effect on WMF and oxygen on contaminants removal by ZVI is under investigation in our lab.

Acknowledgments

This work was supported by the National Natural Science Foundation of China – China (21277095 and 51478329), the Zhejiang Province Natural Science Foundation (LQ15E0 80003), the Shaoxing University of Research Startup Project (20145033), the Specialized Research Fund for the Doctoral Program of Higher Education (20130072110026), and the Tongji University Open Funding for Materials Characterization (2013080). The authors thank beam-lines BL14W1 and BL14B1 (Shanghai Synchrotron Radiation Facility) for providing the beam time.

Appendix A. Supplementary material

Supplementary data associated with this article can be found, in the online version, at http://dx.doi.org/10.1016/j.seppur.2015.09.062.

References

[1] B.P. Rosen, Z. Liu, Transport pathways for arsenic and selenium: a minireview, Environ. Int. 35 (2009) 512–515.
[2] B.D. Gibson, D.W. Blowes, M.B. Lindsay, C.J. Ptacek, Mechanistic investigations of Se(VI) treatment in anoxic groundwater using granular iron and organic carbon: an EXAFS study, J. Hazard. Mater. 241 (2012) 92–100.
[3] J.T. Olegario, N. Yee, M. Miller, J. Sczepaniak, B. Manning, Reduction of Se(VI) to Se(-II) by zerovalent iron nanoparticle suspensions, J. Nanopart. Res. 12 (2010) 2057–2068.
[4] A. Kapoor, S. Tanjore, T. Viraraghavan, Removal of selenium from water and wastewater, Int. J. Environ. Stud. 49 (1995) 137–147.
[5] L. Liang, W. Yang, X. Guan, J. Li, Z. Xu, J. Wu, Y. Huang, X. Zhang, Kinetics and mechanisms of pH-dependent selenite removal by zero valent iron, Water Res. 47 (2013) 5846–5855.
[6] H. Hayashi, K. Kanie, K. Shinoda, A. Muramatsu, S. Suzuki, H. Sasaki, pH-dependence of selenate removal from liquid phase by reductive Fe(II)–Fe(III) hydroxysulfate compound, green rust, Chemosphere 76 (2009) 638–643.
[7] N. Barrow, Testing a mechanistic model. IX. Competition between anions for sorption by soil, J. Soil Sci. 40 (1989) 415–425.
[8] R.H. Neal, G. Sposito, K. Holtzclaw, S. Traina, Selenite adsorption on alluvial soils: I. Soil composition and pH effects, Soil Sci. Soc. Am. J. 51 (1987) 1161–1165.
[9] N. Zhang, D. Gang, L.-S. Lin, Adsorptive removal of parts per million level selenate using iron-coated GAC adsorbents, J. Environ. Eng. 136 (2010) 1089–1095.
[10] Y. Zhang, J. Wang, C. Amrhein, W.T. Frankenberger, Removal of selenate from water by zerovalent iron, J. Environ. Qual. 34 (2005) 487–495.
[11] K. Mondal, G. Jegadeesan, S.B. Lalvani, Removal of selenate by Fe and NiFe nanosized particles, Ind. Eng. Chem. Res. 43 (2004) 4922–4934.
[12] C. Tang, Y.H. Huang, H. Zeng, Z. Zhang, Promotion effect of Mn^{2+} and Co^{2+} on selenate reduction by zero-valent iron, Chem. Eng. J. 244 (2014) 97–104.
[13] C. Tang, Y.H. Huang, H. Zeng, Z. Zhang, Reductive removal of selenate by zero-valent iron: the roles of aqueous Fe^{2+} and corrosion products, and selenate removal mechanisms, Water Res. 67 (2014) 166–174.
[14] A.B. Cundy, L. Hopkinson, R.L.D. Whitby, Use of iron-based technologies in contaminated land and groundwater remediation: a review, Sci. Total Environ. 400 (2008) 42–51.
[15] J.W. Chen, Z.M. Xiu, G.V. Lowry, P.J.J. Alvarez, Effect of natural organic matter on toxicity and reactivity of nano-scale zero-valent iron, Water Res. 45 (2011) 1995–2001.
[16] C. Lee, J.Y. Kim, W.I. Lee, K.L. Nelson, J. Yoon, D.L. Sedlak, Bactericidal effect of zero-valent iron nanoparticles on Escherichia coli, Environ. Sci. Technol. 42 (2008) 4927–4933.
[17] Y. Sun, X. Guan, J. Wang, X. Meng, C. Xu, G. Zhou, Effect of weak magnetic field on arsenate and arsenite removal from water by zero valent iron: an XAFS investigation, Environ. Sci. Technol. 48 (2014) 6850–6858.
[18] L. Liang, W. Sun, X. Guan, Y. Huang, W. Choi, H. Bao, L. Li, Z. Jiang, Weak magnetic field significantly enhances selenite removal kinetics by zero valent iron, Water Res. 49 (2014) 371–380.
[19] L. Liang, X. Guan, Z. Shi, J. Li, Y.-N. Wu, P.G. Tratnyek, Coupled effects of aging and weak magnetic fields on sequestration of selenite by zero-valent iron, Environ. Sci. Technol. 48 (2014) 6326–6334.
[20] I.-H. Yoon, K.-W. Kim, S. Bang, M.G. Kim, Reduction and adsorption mechanisms of selenate by zero-valent iron and related iron corrosion, Appl. Catal. B 104 (2011) 185–192.
[21] C.R. Keenan, D.L. Sedlak, Factors affecting the yield of oxidants from the reaction of nanoparticulate zero-valent iron and oxygen, Environ. Sci. Technol. 42 (2008) 1262–1267.
[22] L.L. Stookey, Ferrozine – a new spectrophotometric reagent for iron, Anal. Chem. 42 (1970) 779–781.
[23] á. Ravel, M. Newville, ATHENA, ARTEMIS, HEPHAESTUS: data analysis for X-ray absorption spectroscopy using IFEFFIT, J. Synchrotron Radiat. 12 (2005) 537–541.
[24] K. Baek, N. Kasem, A. Ciblak, D. Vesper, I. Padilla, A.N. Alshawabkeh, Electrochemical removal of selenate from aqueous solutions, Chem. Eng. J. 215 (2013) 678–684.
[25] D. Burriss, W. Zou, D. Cremer, J. Walrod, D. Atwood, Removal of selenite from water using a synthetic dithiolate: an experimental and quantum chemical investigation, Inorg. Chem. 53 (2014) 4010–4021.
[26] S. Chakraborty, F. Bardelli, L. Charlet, Reactivities of Fe (II) on calcite: selenium reduction, Environ. Sci. Technol. 44 (2010) 1288–1294.
[27] Z. Shi, J.T. Nurmi, P.G. Tratnyek, Effects of nano zero-valent iron on oxidation–reduction potential, Environ. Sci. Technol. 45 (2011) 1586–1592.
[28] L. Liang, X. Jiang, W. Yang, Y. Huang, X. Guan, L. Li, Kinetics of selenite reduction by zero-valent iron, Desalination Water Treat. (2013) 1–9.
[29] A.F. White, M.L. Peterson, Reduction of aqueous transition metal species on the surfaces of Fe(II)-containing oxides, Geochim. Cosmochim. Acta 60 (1996) 3799–3814.
[30] S. Klas, D.W. Kirk, Understanding the positive effects of low pH and limited aeration on selenate removal from water by elemental iron, Sep. Purif. Technol. 116 (2013) 222–229.
[31] H. Wijnja, C.P. Schulthess, Vibrational spectroscopy study of selenate and sulfate adsorption mechanisms on Fe and Al (hydr) oxide surfaces, J. Colloid Interface Sci. 229 (2000) 286–297.
[32] C.-H. Wu, S.-L. Lo, C.-F. Lin, Competitive adsorption of molybdate, chromate, sulfate, selenate, and selenite on γ-Al_2O_3, Colloids Surf., A 166 (2000) 251–259.
[33] S. Sanuki, K. Arai, T. Kojima, S. Nagaoka, H. Majima, Photocatalytic reduction of selenate and selenite solutions using TiO_2 powders, Metall. Mater. Trans. B 30 (1999) 15–20.
[34] R. Singh, V. Misra, R.P. Singh, Synthesis, characterization and role of zero-valent iron nanoparticle in removal of hexavelant chromium from chromium-spiked soil, J. Nanopart. Res. 13 (2011) 4063–4073.
[35] N. Kumar, E.O. Omoregie, J. Rose, A. Masion, J.R. Lloyd, L. Diels, L. Bastiaens, Inhibition of sulfate reducing bacteria in aquifer sediment by iron nanoparticles, Water Res. 51 (2014) 64–72.
[36] C.M. Gonzalez, J. Hernandez, J.G. Parsons, J.L. Gardea-Torresdey, A study of the removal of selenite and selenate from aqueous solutions using a magnetic iron/manganese oxide nanomaterial and ICP-MS, Microchem. J. 96 (2010) 324–329.
[37] D. Peak, D. Sparks, Mechanisms of selenate adsorption on iron oxides and hydroxides, Environ. Sci. Technol. 36 (2002) 1460–1466.
[38] M. Rovira, J. Giménez, M. Martínez, X. Martínez-Lladó, J. de Pablo, V. Marti, L. Duro, Sorption of selenium(IV) and selenium(VI) onto natural iron oxides: goethite and hematite, J. Hazard. Mater. 150 (2008) 279–284.
[39] D. Peak, Adsorption mechanisms of selenium oxyanions at the aluminum oxide/water interface, J. Colloid Interface Sci. 303 (2006) 337–345.
[40] M. Martinez, J. Gimenez, J. De Pablo, M. Rovira, L. Duro, Sorption of selenium (IV) and selenium(VI) onto magnetite, Appl. Surf. Sci. 252 (2006) 3767–3773.
[41] Y. Fu, J. Wang, Q. Liu, H. Zeng, Water-dispersible magnetic nanoparticle–graphene oxide composites for selenium removal, Carbon 77 (2014) 710–721.
[42] S. Das, M. Jim Hendry, J. Essilfie-Dughan, Adsorption of selenate onto ferrihydrite, goethite, and lepidocrocite under neutral pH conditions, Appl. Geochem. 28 (2013) 185–193.

[43] W.H. Kuan, S.L. Lo, M.K. Wang, C.-F. Lin, Removal of Se (IV) and Se (VI) from water by aluminum-oxide-coated sand, Water Res. 32 (1998) 915–923.
[44] C.M. Gonzalez, J. Hernandez, J.R. Peralta-Videa, C.E. Botez, J.G. Parsons, J.L. Gardea-Torresdey, Sorption kinetic study of selenite and selenate onto a high and low pressure aged iron oxide nanomaterial, J. Hazard. Mater. 211 (2012) 138–145.
[45] Y.H. Huang, T.C. Zhang, Reduction of nitrobenzene and formation of corrosion coatings in zerovalent iron systems, Water Res. 40 (2006) 3075–3082.
[46] E.J. Elzinga, Y. Tang, J. McDonald, S. DeSisto, R.J. Reeder, Macroscopic and spectroscopic characterization of selenate, selenite, and chromate adsorption at the solid–water interface of γ-Al_2O_3, J. Colloid Interface Sci. 340 (2009) 153–159.
[47] M. Kang, B. Ma, F. Bardelli, F. Chen, C. Liu, Z. Zheng, S. Wu, L. Charlet, Interaction of aqueous Se(IV)/Se(VI) with FeSe/$FeSe_2$: implication to Se redox process, J. Hazard. Mater. 248 (2013) 20–28.